

# MODELING OF HYDROGEN EXPLOSION ON A PRESSURE SWING ADSORPTION FACILITY

B. Angers<sup>1</sup>, A. Hourri<sup>1</sup>, P. Benard<sup>1</sup>, E. Demaël<sup>2</sup>, S. Ruban<sup>2</sup>, S. Jallais<sup>2</sup>

<sup>1</sup> Institut de recherche sur l'hydrogène, Université du Québec à Trois-Rivières, Québec, Canada, Benjamin.Angers@uqtr.ca, Ahmed.Hourri@uqtr.ca, Pierre.Benard@uqtr.ca

<sup>2</sup> Air Liquide, Centre de Recherche Claude-Delorme, 78350 Jouy en Josas, France

## ABSTRACT

This article presents a numerical study of the consequences of an hydrogen release from a pressure swing adsorption installation operating at 30 barg. The simulations are performed using FLACS/Hydrogen from GexCon. The impact of obstruction, partial confinement, leak orientation and wind on the explosive cloud formation (size and explosive mass) and on explosion consequences is investigated. In parallel, overpressures resulting from ignition are calculated as a function of the time to ignition.

## 1.0 INTRODUCTION

The overpressures associated with an hydrogen cloud ignition represent a significant hazard for large scale hydrogen production facilities. In the event of an unintentional ignition, the presence of many obstacles and the high degree of confinement inherent to these facilities greatly increase the risk of higher flame velocities which in turn generate overpressure waves. The study of these hazards is of significant interest to hydrogen suppliers in order to establish and validate mitigation procedures [1,2].

In this context, we investigate the impact of confinement and turbulence inducing mechanisms, such as wind and obstacles, on the overpressure generated during the combustion of a hydrogen gas cloud arising from a Pressure Swing Adsorption (PSA) facility. Dispersion simulation results for a jet release from three 30.4 barg reservoirs using the commercial FLACS/Hydrogen program are presented. The simulation scenarios considered are two hydrogen leaks from orifices with diameters 20 mm and 35 mm in a still environment (without wind) and in windy environment where the wind velocities are 3 m/s and 5 m/s. For each scenario, two hydrogen jet directions have been considered. In the first case, the jet was oriented such that it impinges on the ground with an angle of 45° and in the second case, the jet was directed horizontally. Critical profiles of hydrogen concentration in air are presented. We also present multiple scenarios where the jet is ignited close to the ground. The overpressure resulting from the cloud ignition is estimated as a function of the leak direction and time to ignition.

## 2.0 MODELLING SCENARIO DESCRIPTION

As shown in Figure 1, the PSA installation consisted of 12 linked pressurized pipes. The average distance (pitch) between adjacent pipes is presented in Table 1. The pitch was measured center to center minus the radius of adjacent pipes. Only pipes with a radius of more than 0.168 m were considered for the pitch calculation. The volume blockage ratio (VBR), area blockage ratio (ABR) and the piping surface area per volume for different regions of the installation are given in Table 2. The VBR and ABR are respectively defined as the percentage of volume and surface blocked by objects in a given region. The piping surface area per volume given by FLACS *cofile* utility is defined as the objects surface area divided by the volume of the region considered. Figure 2 and Figure 3 show volumes and areas used for the VBR, ABR and piping surface area calculation.

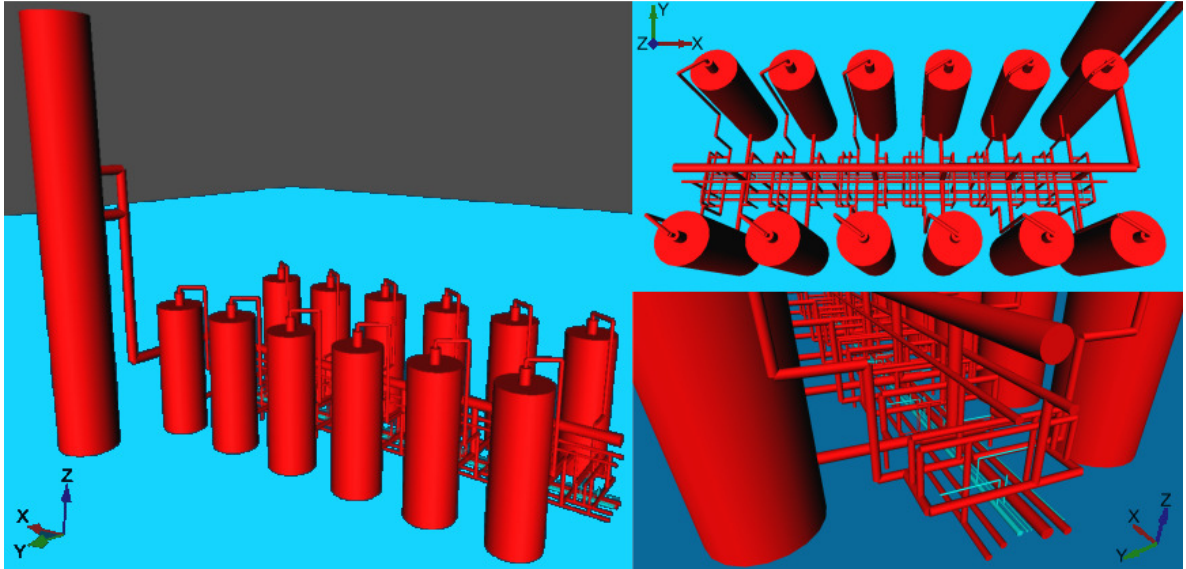


Figure 1. Pressure swing adsorption installation (PSA) viewed from different angles.

Table 1. The average distance (pitch) between pipes inside the central region of the PSA in each direction

Direction	X	Y	Z
Pitch (m)	0.52	0.37	0.65

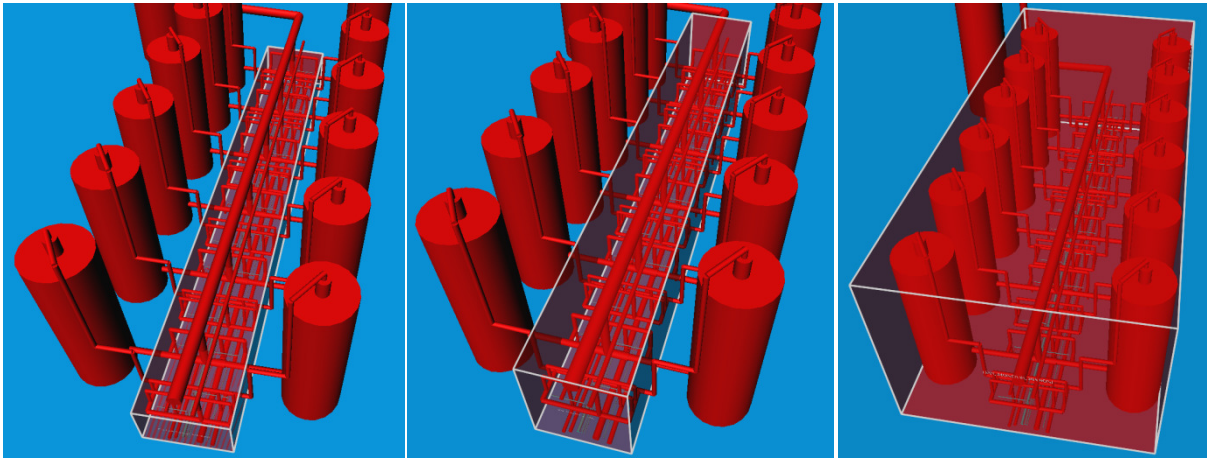


Figure 2. Each box shows the volume used to calculate the VBR of the central region on the left, the central wide region in the middle and the reservoir region on the right.

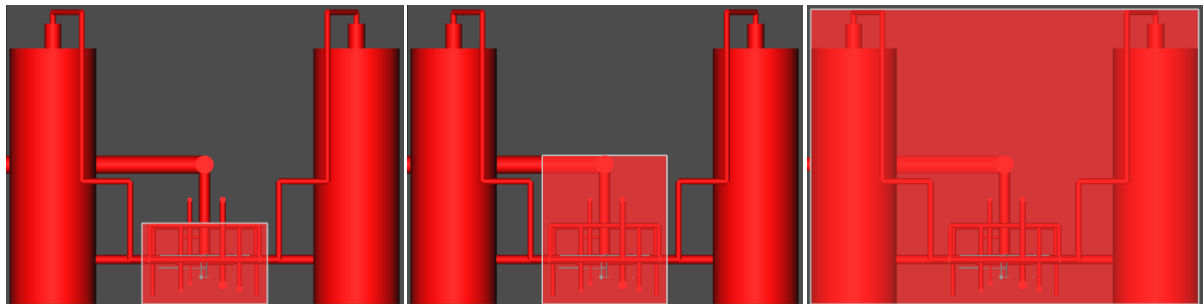


Figure 3. The left, middle and right picture show the area used to calculate the central, the central wide and the reservoir ABR respectively.

Table 2. Volume blockage ratio (VBR), area blockage ratio (ABR) and piping surface area

Region	Central	Central wide	Reservoir
Total volume (m3)	403.8	741.1	4572.6
PSA volume (m3)	19.2	33.6	873.3
VBR (%)	4.8	4.5	19.1
Total area (m2)	13.1	24.0	148.0
PSA area (m2)	4.8	6.3	68.2
ABR (%)	36.5	26.2	46.1
Piping surface area (m2)	93.9	116.6	784.1
Piping surface area per volume (m2/m3)	0.233	0.157	0.171

The leak was assumed to originate from a broken branch connection at one end of the system. The position of the leak is shown in Figure 4. Three of the 43.3 m<sup>3</sup> reservoirs contain hydrogen at a pressure of 30.4 barg and at a temperature of 45°C. The leak diameters considered, i.e. 20 mm and 35 mm, correspond to a rupture at a branch connection of 3/4" and 1"1/2 respectively. As a conservative approximation, the pressure drop through the pipes from the reservoirs to the leak was not taken into account.

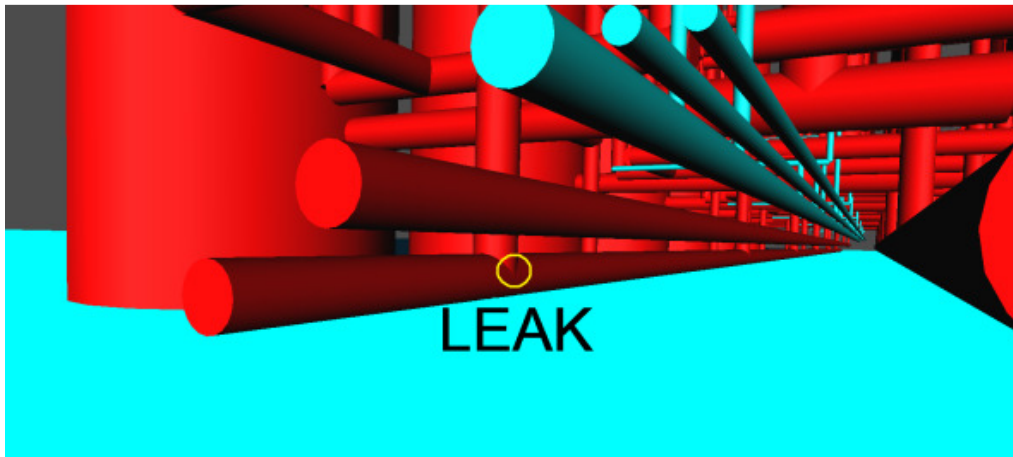


Figure 4. A branch connection was selected as leak origin. The leak is located 0.5 m above the ground.

For clarity, the following nomenclature was used to define the different scenarios: **35NW45°C2** means that the leak diameter is **35** mm, there is **No Wind**, the jet direction is set **45°** toward the ground, it is a **Combustion** simulation and the time to ignition is set at **2** sec after the leak onset. The jet cloud ignition was assumed to occur on the ground inside the 30% concentration envelop. For most simulations, the cloud was ignited 2 seconds and 20 seconds after the leak onset. At 2 seconds, the cloud is small but contains a higher concentration of hydrogen, while at 20 seconds, the cloud is well developed but more diluted and it covers most of the PSA. In one case (35NW45°), the time to ignition was varied between 0.5 second and 60 seconds. For the scenarios with wind, the atmospheric stability Pasquill class F was chosen for 3 m/s wind, and class D for 5 m/s wind. In these cases, the reference height was set at 10 m and the ground roughness at 0.03 m (open flat terrain; grass, few isolated obstacles). The wind direction was the same as that of the jet.

FLACS uses a rectilinear grid. In the case of jet dispersion, a zone made of cubic cells was defined at the expanded jet location. Following Gexcon good practice recommendations [3], the cell size of the initial cubic zone at the expanded jet location was determined by the effective leak area  $A_{leak}$  so that  $A_{cv} > A_{leak} > 0.9A_{cv}$  where  $A_{cv}$  is the area of the control volume. The leak originates from one cell in the initial cubic zone. From that initial zone, the grid was stretched to a coarser cubic grid encompassing the PSA. The size of the central region cells encompassing the PSA was set at 0.5 m for

both dispersion and combustion grids. It was then stretched again outside the PSA to a coarser rectangular grid. One grid was used for all combustion simulations.

Combustion grid dependency studies were done for the windless case scenario with 35 mm leak diameter directed 45° toward the ground at 20 seconds, by setting the size of the central region cells encompassing the PSA to 0.25 m. In this case, the difference in the maximum overpressure does not exceed 18% and -4% in the domain and on the monitor points when respectively compared with the overpressures obtained with 0.5 m cells. On the other hand, with an ignition time of 2 seconds the maximum overpressure was lowered with 0.25 m cells by -29% and -34% in the domain and on the monitor points when respectively compared with the overpressures obtained with 0.5 m cells. Gexcon recommend that the reactive flammable cloud be resolved with a minimum of 10 grid cells in the direction where the cloud meets confinement. Due to our choice of using the same grid for all the combustion simulations, this rule was broken in the cases where the ignition time was lower.

For each scenario, the flow is choked at the jet exit. The jet outlet conditions, i.e. the leak rate, temperature, effective leak area, velocity and the turbulence parameters (i.e. turbulence intensity and turbulent length scale) for the flow, are calculated using an imbedded jet program in FLACS. FLACS can also calculate the time dependent leak and turbulence parameters for continuous jet releases in the case of high pressure vessel depressurization. The estimate assumes isentropic flow conditions through the nozzle, followed by a single normal shock (whose properties are calculated using the Rankine-Hugoniot relations), which is subsequently followed by expansion into ambient air [4].

For the 20 mm and 30 mm leak diameter, the initial mass flow rate was 0.502 kg/s and 1.539 kg/s respectively. A discharge coefficient of 0.85 was used.

Overpressure measurements were taken at regular intervals along and perpendicular to the jet direction. Monitoring points were positioned on the ground and 1.0 m above the ground as shown on Figure 5.

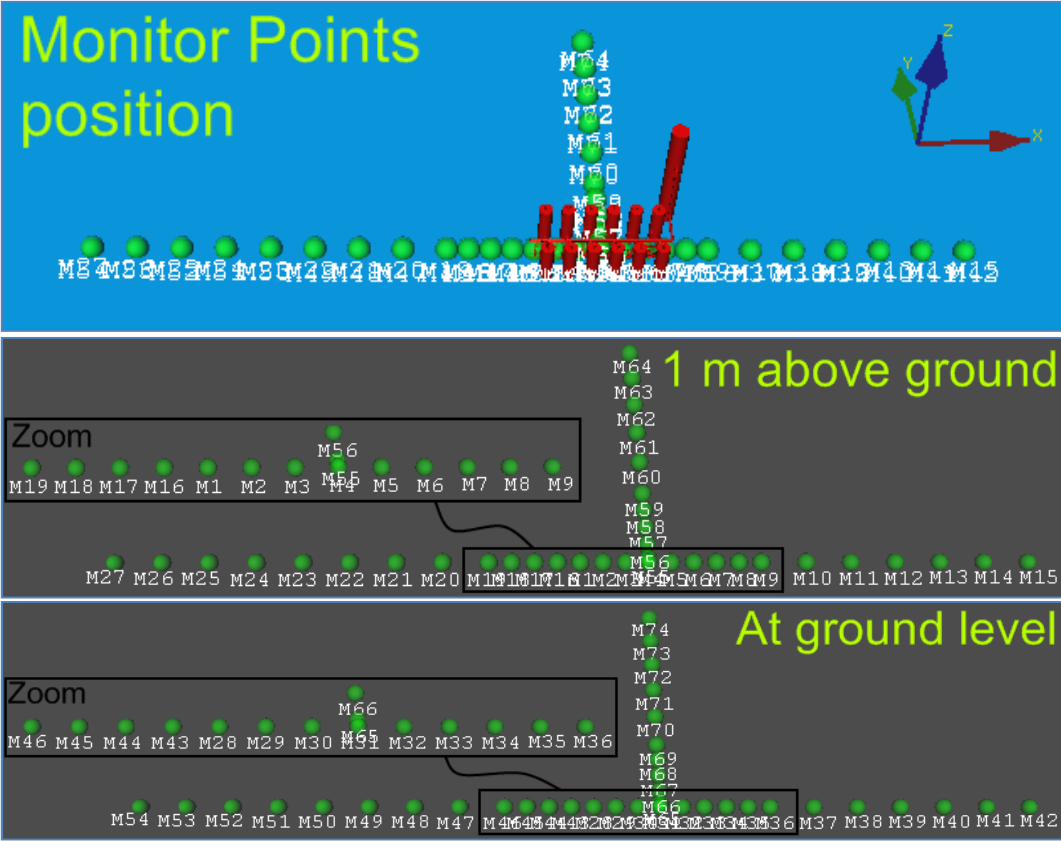


Figure 5. Monitoring points position

### 3.0 MODELING RESULTS

Figure 6 shows the transversal cut going vertically along the axis of the jet through the hydrogen flammable contour (at the lower flammability limit (LFL): 4% molar fraction  $H_2$  in air) at 2 seconds and 20 seconds after the leak onset for the dispersion scenarios where  $d = 35$  mm.

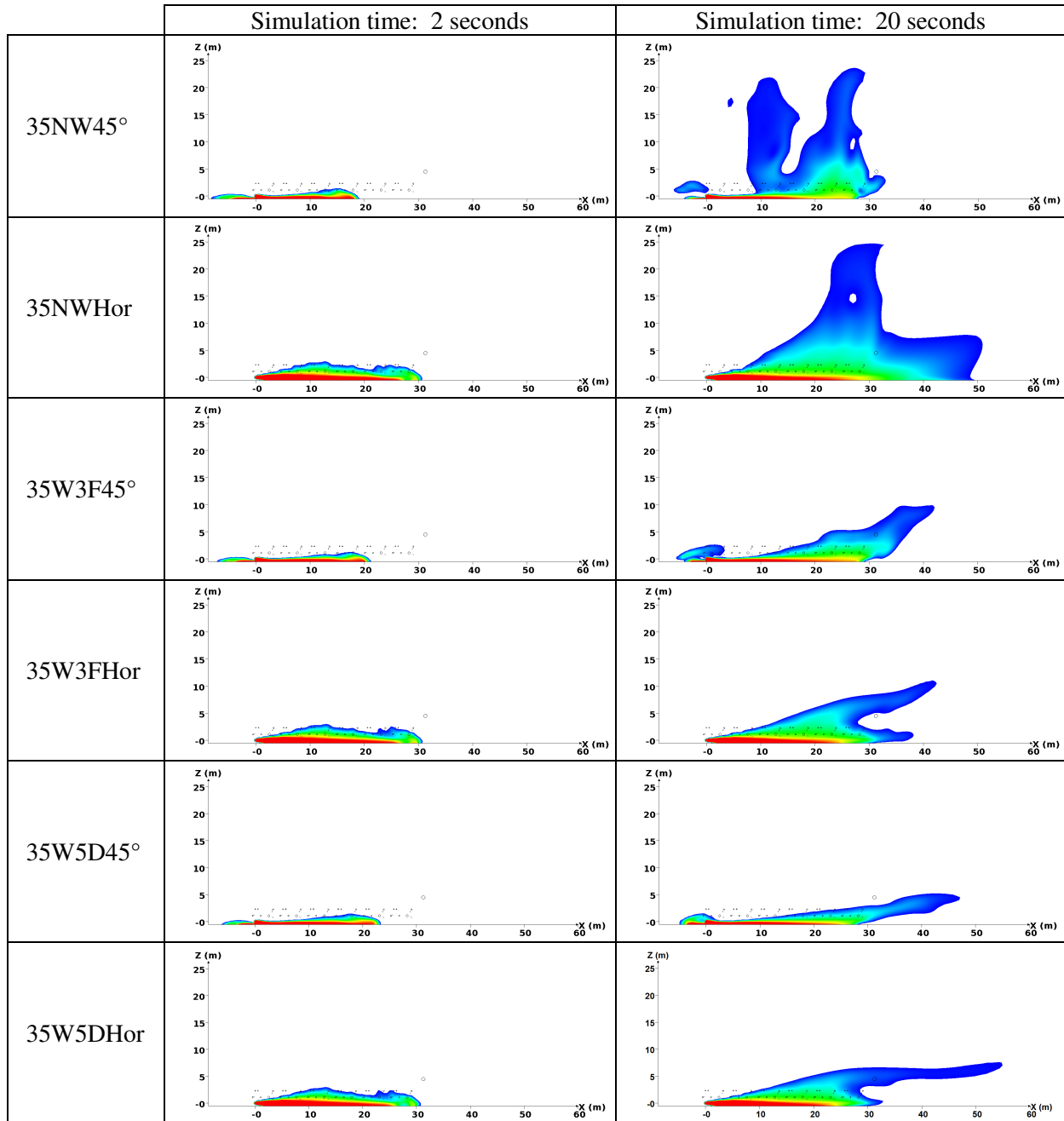


Figure 6. Hydrogen molar concentration envelop profile (up to 30% in red) of the lower flammability limit contour (4% in blue) along the jet direction ( $Y = 0$  m) for a leak diameter of 35 mm.

As shown on Figure 6 for similar cases, the wind does not influence significantly the shape of higher concentrations contours (red zones near the ground). On the other hand, the lower concentrations contours are greatly affected by the wind. They extend horizontally instead of dispersing upward when wind is present.

Figure 7 shows the mass histogram taken from the combustion grid for the 35NW45° scenario at 2 sec and 20 sec. Flammable mass at 2 sec release time is lower (near 3 kg) than at 20sec (near 12kg).

However, the flammable cloud is more concentrated in hydrogen at 2 sec compared to 20 sec and is then more reactive. Figure 8 presents the maximum overpressures measured during a series of combustion simulations based on the same scenario (35NW45°) where the time to ignition was varied from 0.5 sec to 60 sec. As shown, these overpressures were measured at the monitoring points as well as in the entire domain. Figure 8 also shows the hydrogen mass at stoichiometric concentration, right before the cloud was ignited. It should be noted that we could not extract from FLACS the hydrogen mass at stoichiometric concentration. We can only extract mass values from concentration intervals. However, an approximate of the stoichiometric mass of hydrogen extracted from the interval 28-32% (vol.) was plotted in Figure 8 as a function of time to ignition. Overpressure and hydrogen mass at stoichiometric concentration peaks are observed at 2 sec and 20 sec as illustrated in Figure 8.

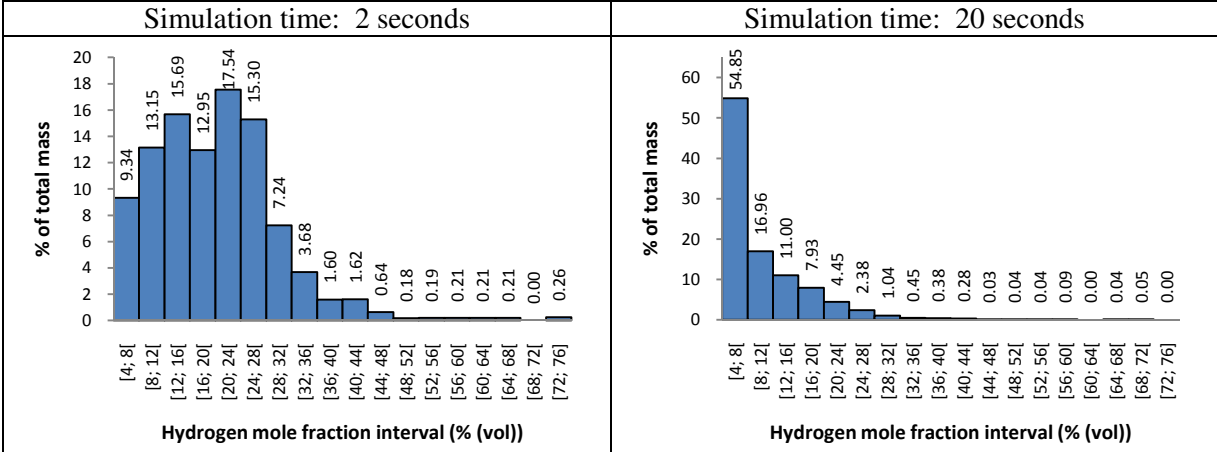


Figure 7. Mass histogram from combustion grid, prior to ignition for the 35NW45° scenario.

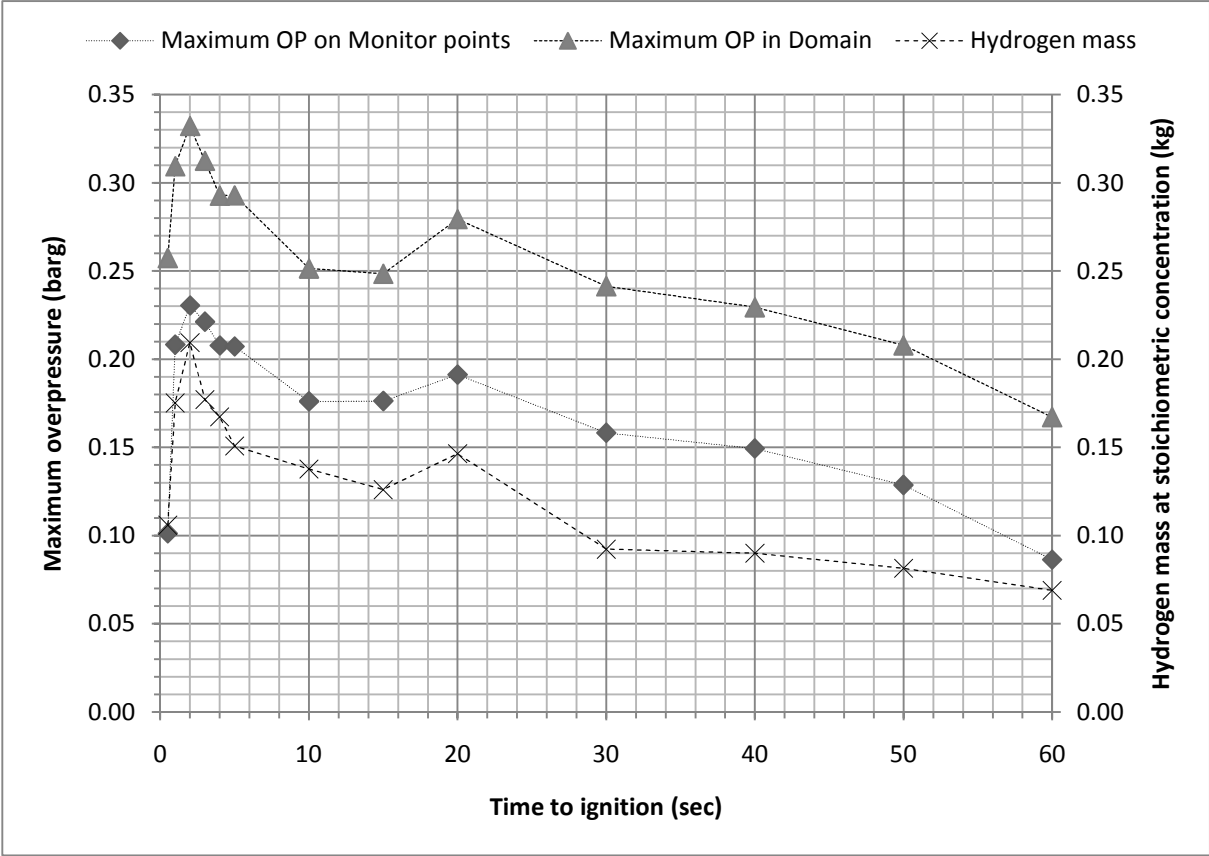


Figure 8. Maximum overpressure and hydrogen mass at stoichiometric concentration (between 28-32% (vol.)) as a function of time to ignition for the 35NW45° scenario.

The relation between time to ignition and maximum overpressure was thoroughly studied [5]. As shown on Figure 8, the highest overpressure was measured with a time to ignition of 2 sec in agreement with the experimental findings of Takeno *et. al.* [6] who concluded that short time to ignition resulted in higher overpressure. Royle *et. al.* [7] observed the same phenomena in their experiment. As shown on Figure 7, while the total amount of flammable fuel is lower at 2 sec (2.98 kg) than at 20 sec (14.19 kg), the hydrogen mass at stoichiometric concentration is higher at 2 sec (0.21 kg) than at 20 sec (0.15 kg). Note also on Figure 8 that the peaks in hydrogen mass at 2 sec and at 20 sec follow the same trend as the maximum overpressures. Figure 9 shows the flammable mass of hydrogen at two concentrations intervals: 4-75% and 11-75%. The 11 – 75% interval is useful because it correspond to the hydrogen concentrations for which a strong flame acceleration is observed by Dorofeev [8]. For both intervals, the flammable mass reaches a maximum at 20 sec.

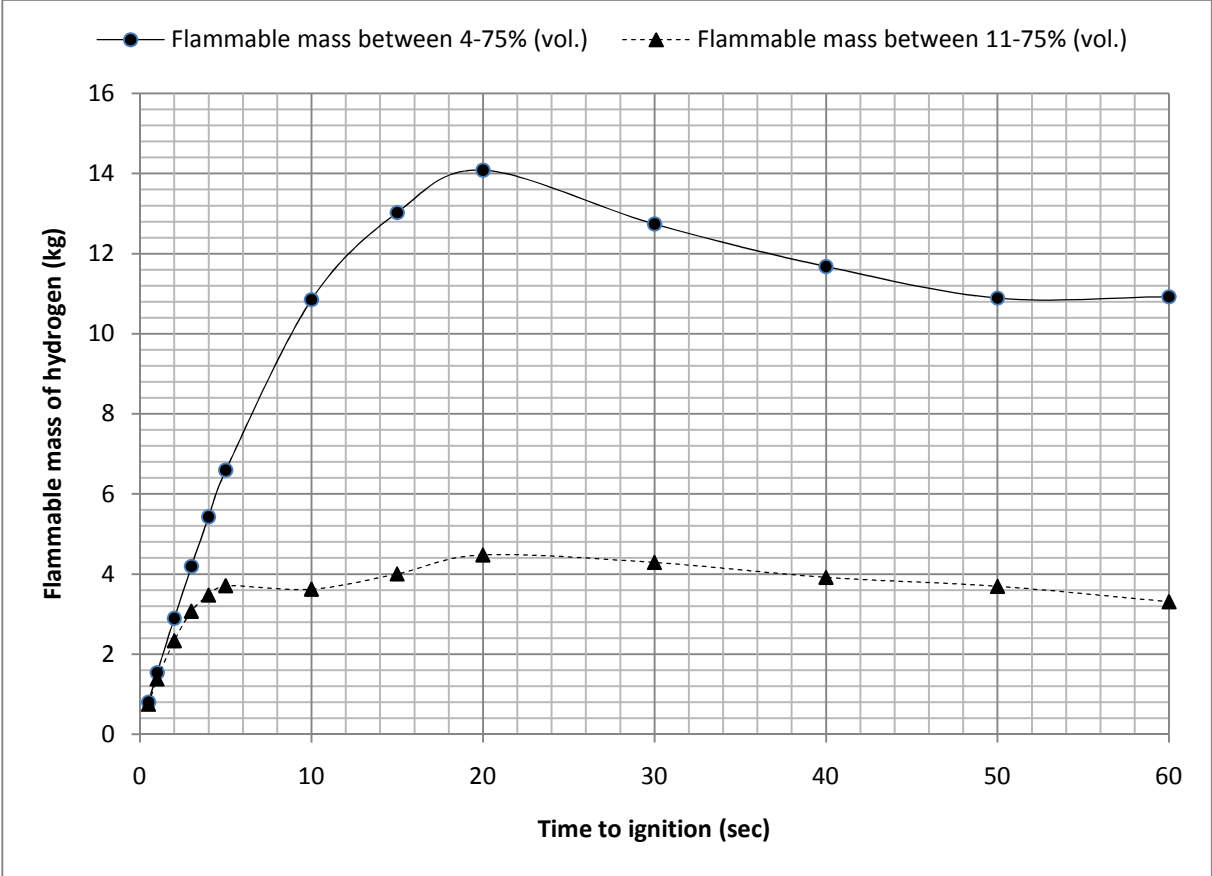


Figure 9. Flammable mass of hydrogen between mole fraction intervals of 4-75% (vol.) and 11-75% (vol.), right before the cloud was ignited, as a function of time to ignition for the 35NW45° scenario.

The maximum overpressures for all combustion simulations are presented in Figure 10 and Figure 11. As shown on Figure 10, maximum overpressures were 5 to 6 times more powerful for horizontal jets than for the 45° jets. We see the same trend on Figure 11 for maximum overpressures measured on monitor points, although the ratio is only 2. As shown on Figure 6, in the horizontal case, most of the stoichiometric concentration contours are near the ground under the PSA. The most reactive part of the cloud is outside the congested area where most of the pipes accelerating the flame are. This is particularly true for jets with  $d = 20$  mm and for jets oriented 45° toward the ground. On the other hand, the flammable concentration envelop encompasses the congested area much more for the horizontal jet than for the 45° jets.

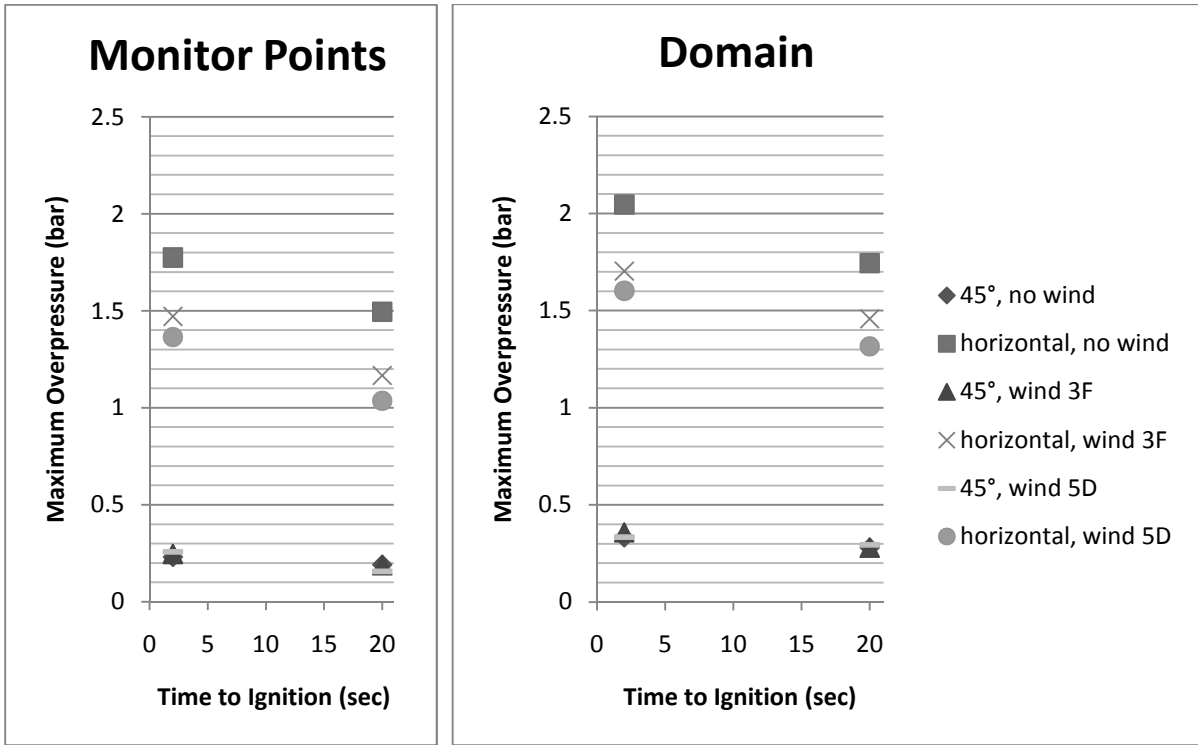


Figure 10. Maximum overpressure as a function of time to ignition measured on all monitor points and in the domain for simulations with  $d = 35$  mm.

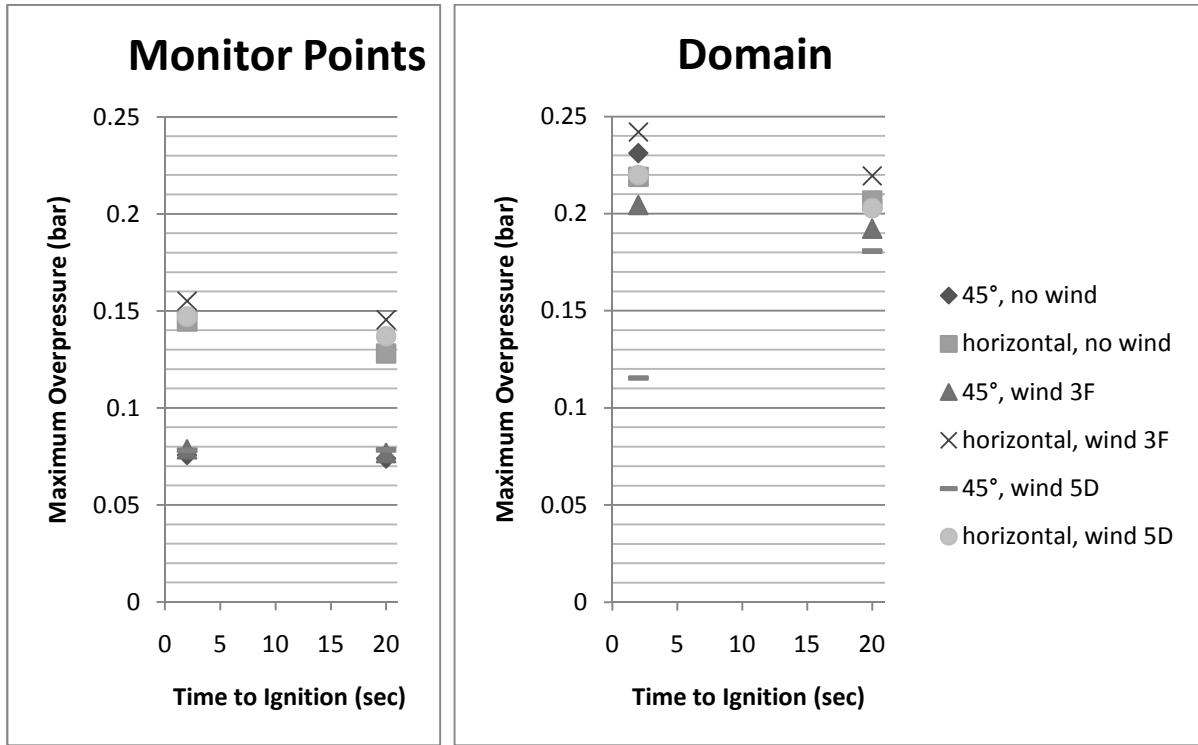


Figure 11. Maximum overpressure as a function of time to ignition measured on all monitor points and in the domain for simulations with  $d = 20$  mm.

Overpressure extents at 50 mbar, 140 mbar and 200 mbar are given in Figure 12. Isocontours on the XZ view plane (along jet axis) and XY view plane (1 m above ground) for the scenario (35NW45°) at 50 mbar are shown on Figure 13, at various times after ignition.



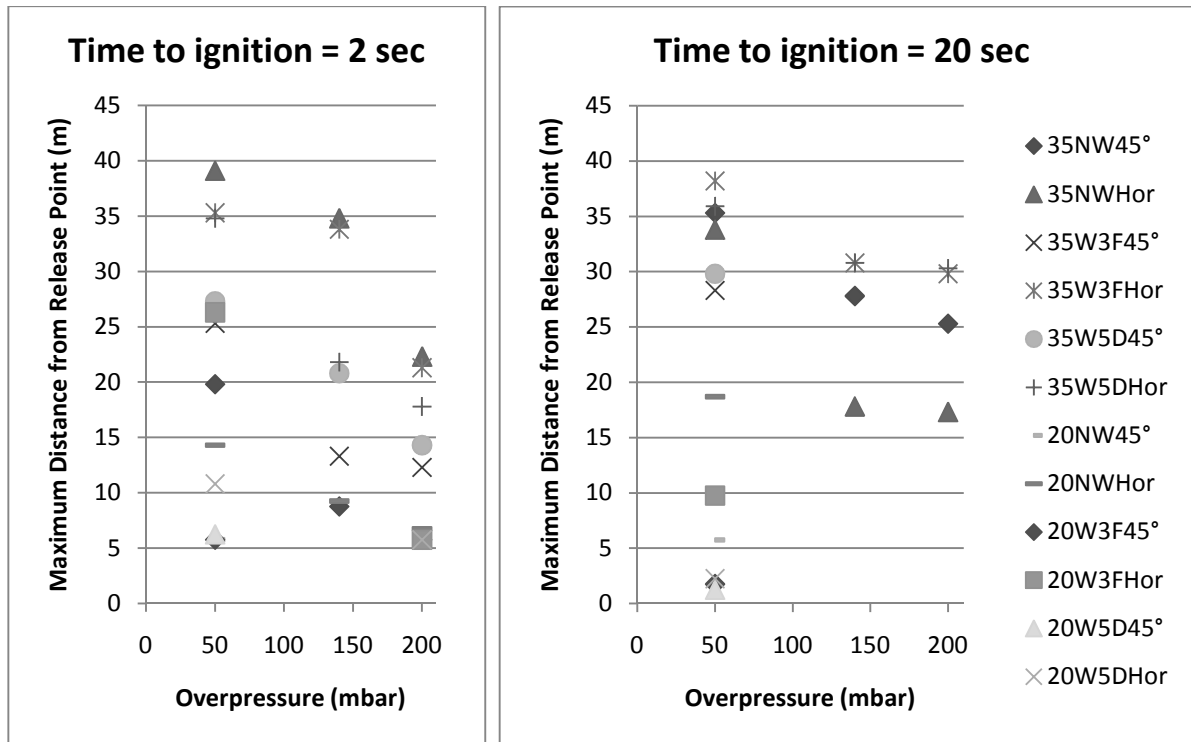


Figure 12. Maximum travel distance of 50 mbar, 140 mbar and 200 mbar overpressure fronts measured from the origin of the leak at (0, 0, 0).

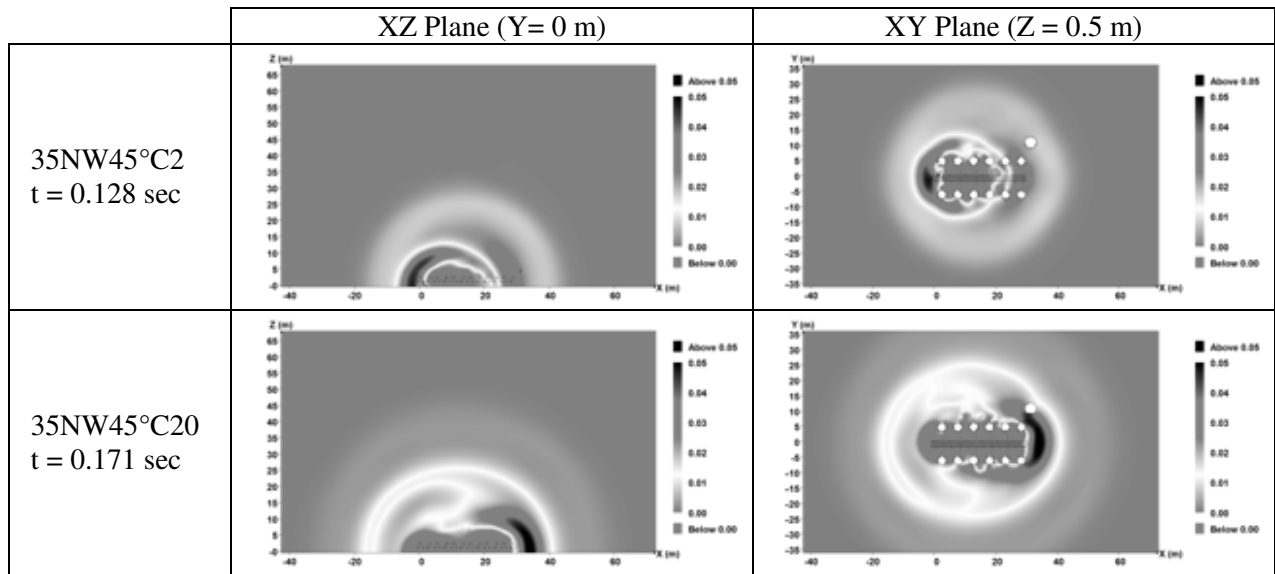


Figure 13. 50 mbar isocontours at various times after ignition on the XZ plane (along jet axis) and XY plane (1 m above ground) for the 35NW45° scenario.

For the 45° angle release with the 35 mm hole, even if the cloud is more reactive at 2 sec, the safety distances are lower than in the 20 sec case. At the opposite, in the horizontal release, these safety distances become larger at 2 sec compared to 20 sec case due to the entire flame propagation in the congested part of the PSA.

## 4.0 CONCLUSION

We presented results of finite volume simulations for a time-dependent hydrogen release from a broken branch connection 0.5 m above the ground, originating from three 43.3 m<sup>3</sup> reservoirs at 30.4 barg of a pressure swing adsorption installation. An overpressure of 0.33 bar was obtained with a leak diameter of 35 mm oriented 45° toward the ground, with no wind. For all scenarios, a maximum overpressure of 2.05 bar was obtained with a leak diameter of 35 mm, oriented horizontally, with no wind, when ignited 2 sec after the leak onset. For the same scenario, a 50 mbar pressure wave travelled up to 40 m in the direction of the leak and 26 m perpendicular to it.

The effects of a 3 m/s and 5 m/s wind were considered. In the presence of a 3m/sec Pasquill class F wind, a maximum overpressure of 1.70 bar was obtained with a leak diameter of 35 mm, oriented horizontally and ignited 2 sec after the onset of the leak. In this case, the 50 mbar pressure wave travelled 35 m along the jet axis and 24 m perpendicular to the jet.

Two orifice diameters were considered in this study, namely 20 mm and 35 mm. An average maximum overpressure of 0.20 bar was obtained for most scenarios with  $d = 20$  mm. On the other hand, with  $d = 35$  mm, the maximum overpressure varied from 0.28 bar up to 2.05 bar depending on the jet orientation, wind strength and ignition time.

The consequences of ignition shortly after the start of the release were also presented. The time of ignition was varied from 0.5 sec to 60 sec for one case. Short time to ignition usually results in higher overpressure, based on the amount of hydrogen at stoichiometric concentration. This was mainly noticeable for the simulations with  $d = 35$  mm, less with  $d = 20$  mm.

## ACKNOWLEDGEMENTS

We gratefully acknowledge the support of Air Liquide. We thank Olav Roald Hansen of GexCon for useful discussions. We also thank Fernando Gomez, Tommy Henly from IRH for their help with the geometry importation and the programming of data analysis tools.

## REFERENCES

1. B. Angers, A. Hourri, P. Bénard, P. Tessier and J. Perrin, Simulation of Hydrogen Releases from a High Pressure Reservoir : Dispersion and Consequences of Ignition. Proceedings of the International Conference on Hydrogen Safety 2005, Pisa, Italy.
2. Hourri, A., Angers, B., Bénard, P., Surface effects on flammable extent of hydrogen and methane jets, International Journal of Hydrogen Energy, 2009; 34: 1569-1577.
3. FLACS V9 User's guide, Gexcon, 2009.
4. Houf, W., Winters, W., Evans, G., Approximate Inflow Conditions for Subsonic Navier-Stokes Computations of Under-Expanded Jets, Unpublished manuscript.
5. Angers, B., Hourri, A., Bénard, P., Hydrogen dispersion and ignition from high pressure storage systems, IRH, Report, July 2007.
6. Takeno K., Okabayashi K., Ishinose T., Koushi A., Nokana T., Hashiguchi K. and Chitose K.: Phenomena of dispersion and explosion of high pressurized hydrogen, Proceedings of the International Conference on Safety 2005, Pisa, Italy.
7. M. Royle, D.B. Willoughby, Consequences of catastrophic releases of ignited and unignited hydrogen jet releases, International Journal of Hydrogen Energy, 2011; 36: 2688-2692.
8. S. B. Dorofeev Flame acceleration and explosion safety applications, Proceedings of the Combustion Institute, Volume 33, Issue 2, 2011, Pages 2161-2175.